Models for the Yielding Behavior of Amorphous Solids

Srikanth Sastry*
Jawaharlal Nehru Centre for Advanced Scientific Research, Jakkur Campus, Bengaluru 560064, India

(Received 11 December 2020; accepted 18 May 2021; published 22 June 2021)

Investigations of plastic deformation and yielding of amorphous solids reveal a strong dependence of their yielding behavior on the degree of annealing. Above a threshold degree of annealing, the nature of yielding changes qualitatively, becoming progressively more discontinuous. Theoretical investigations of yielding in amorphous solids have almost exclusively focused on uniform deformation, but cyclic deformation reveals intriguing features that remain uninvestigated. Focusing on athermal cyclic deformation, I investigate a family of models, which reproduce key features observed in simulations, and provide an interpretation for the intriguing presence of a threshold energy.

DOI: 10.1103/PhysRevLett.126.255501

Amorphous solids of a wide variety are of scientific and technological importance. Apart from *hard* glasses such as oxide glasses, metallic glasses, etc., the broad spectrum of amorphous solids also includes *soft* materials such as colloidal assemblies, gels, emulsions, and pastes [1,2]. How such solids respond to external stresses is equally diverse, understanding which is of interest for many reasons—whereas plastic deformation leading to mechanical failure may be a phenomenon to predict and prevent for structural materials, controlling elastoplastic *flow* properties is of interest in the case of soft materials [1]. A general description of the mechanical response of amorphous solids needs to take note of the microscopic structural disorder and account for the apparent diversity of responses.

The nature of elementary processes of plasticity, interactions between them, the nature of the yielding transition, and the dependence of the mechanical response on preparation history, have been actively investigated over the years [3–16]. In particular, computer simulations of athermal quasistatic shear deformations [11–13,17–20], employing both uniform and cyclic shear protocols, reveal that the character of yielding depends strongly on the initial degree of annealing of the solid. Under uniform shear, the evolution of stress with strain is gradual for poorly annealing glasses, whereas well annealed glasses display both a stress overshoot and a discontinuous jump down to the flow stress, with the strength of discontinuity growing with annealing, above a threshold degree of annealing. Such variation of yielding behavior with annealing has been suggested as a framework to understand the observed diversity among amorphous solids [12].

In the case of cyclic shear, poorly annealed glasses, above a threshold energy (or equivalently, *below* a threshold degree of annealing), anneal toward a threshold energy with increasing amplitude of strain, before yielding [11,13,18], accompanied by shear banding [21] (as also for uniform shear). Initially well annealed samples with energies below the threshold do not show any appreciable change in properties until they yield discontinuously. Above yielding, the properties do not depend on the initial sample history. Interestingly, the number of cycles required to reach the steady state increases strongly as the strain amplitude approaches, and possibly diverges at, the yielding amplitude [6,11,22]. These features are schematically summarized in Fig. 1.

Based on the observations that plastic deformation involves spatially localized arrangements (termed shear

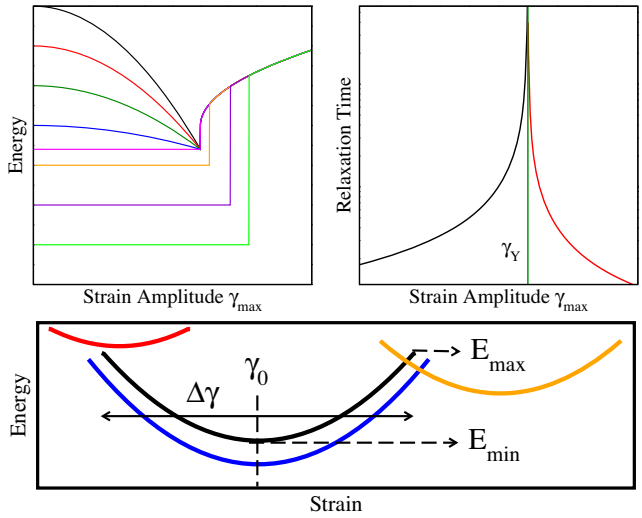

FIG. 1. (Top) Schematic representation of yielding behavior under cyclic shear. (Left) Dependence of steady state energy on strain amplitude γ_{max} for different initial energies. (Right) Time required to reach the steady state vs strain amplitude γ_{max}. (Bottom) A schematic description of the model. The minimum (E_{min}) and maximum (E_{max}) energy, strain at which energy is minimum (γ_0) and the stability range ($\Delta\gamma$) are indicated for one mesostate (black), from which transitions are possible to two other mesostates shown (blue, orange) but not to the third (red).

transformation zones), and that they lead to the generation of long range stress fields, a variety of *elastoplastic* models [2] have been developed and studied, aiming to capture macroscopic deformation response, through a combination of a coarse-grained description of local plasticity, and a continuum description at larger length scales. Attempts have been made to incorporate the role of annealing in such models, for uniform shear [12,15,16,23], but response to cyclic shear remains largely unaddressed. In particular, features exhibited by athermal cyclic shear, including mechanically induced aging or annealing, the presence of a threshold energy across which the character of yielding changes, the apparent divergence of timescales have not been demonstrated to arise in such models. One may well demand that a satisfactory elastoplastic model be able to capture such phenomena, capture both athermal and thermal effects, and have the potential to parametrically incorporate material specific properties. The ability to capture memory effects seen in cyclically sheared glasses would be another desirable feature [24,25]. Such expectations point to an energy based model [26–29] (such as the soft glassy rheology or SGR model [26]), rather than models defined in terms of threshold stresses, as with typical elastoplastic models.

The models studied here are defined in terms of the distribution of states or energy minima that a mesoscale block of an amorphous solid can be in, and rules for transitions between them. Inclusion of an extended array for such blocks and interactions between them along previously developed lines [2] is an obvious next step but is not pursued here. Each state (termed a *mesostate* and investigated in detail in [25]) is characterized by (i) an energy E_0 (taken to be negative always) at a strain value γ_0 at which the energy is minimum, (ii) a stability range in strain over which it is stable, and (iii) a form for the variation of the energy with strain (see Fig. 1 for an illustration). These characterizations can be made in principle in material specific ways. Here, I choose the stability range to be $\gamma_\pm = \gamma_0 \pm \sqrt{-E_0}$, and the energy at a given strain within the stability range as $E(\gamma, E_0, \gamma_0) = E_0 + (\mu/2)(\gamma - \gamma_0)^2$. These choices embody the expectation (supported by numerical evidence [13]) that the stability range as well as the elastic energy rise before instability increase upon lowering the minimum energy. I consider a Gaussian distribution of energies, $P_0(E_0) = \sqrt{2/\pi\sigma^2} \times \exp(-E_0^2/2\sigma^2)$, for $-1 < E_0 < 0$, $\sigma = 0.1$ [30,32].

For a given energy E_0, it is assumed that one has mesostates with several possible values of the *stress-free* strain γ_0, reflecting the fact that distinct configurations of the same energy may exist, with different strain values at which they are stable [33]. For concreteness, two specific cases are considered here: (1) The *regular* case, where mesostates have $\gamma_0 = n \times 2\sqrt{-E_0}$, n being an integer, so that mesostates at a given energy are present in a periodic, nonoverlapping fashion. (2) The *uniform* case, where the γ_0 values are uniformly distributed.

When the stability limit $\gamma_\pm$ is reached, the state of the system makes a transition from the current mesostate to another. In the athermal case, clearly, such a transition is possible only to other states with lower energy at the same strain value (see Fig. 1). Depending on the E_0 and γ_0 values of the other states, a transition may occur to mesostates with higher or lower E_0, a key feature for the behavior described below. One may consider a transition rule that permits transitions to (i) *any* mesostate with a lower energy at the transition strain, or as a physically motivated choice, (ii) restrict the range of E_0 values to which transitions are permitted, within a range δE. Both these cases are considered.

The case of regular distribution of γ_0 is considered first, with a choice of $\mu = 1.1$. The evolution of the system as strain is varied involves a deterministic variation of energy according to the expression for $E(\gamma, E_0, \gamma_0)$ above, and a stochastic change in state when the mesostate becomes unstable upon reaching the strain values $\gamma_\pm$. This evolution is investigated numerically as follows. Starting with an initial energy E_0, and $\gamma_0 = 0$, the strain γ is varied cyclically with amplitude $\gamma_{\max}$, and the state of the system is propagated until a stability limit $\gamma_\pm$ is reached. When this happens, the set of all states to which a transition can occur, with the corresponding weights [given by $P_0(E_0)$; in practice, the E_0 range is divided into 10^4 bins] is evaluated, and a new state, with its E_0 and γ_0 values, is randomly chosen among permitted states. The procedure is repeated for 10^3 cycles of shear. If the state of the system does not change at the end of successive cycles, the procedure is terminated. Otherwise, the zero strain energies for the last 200 cycles are averaged. This procedure is repeated for 10^3 independent sample runs. Figure 2(a) shows the resulting final energies as a function of both a set of initial energies and strain amplitudes. Strikingly, all the essential observations from simulations are reproduced. For high initial

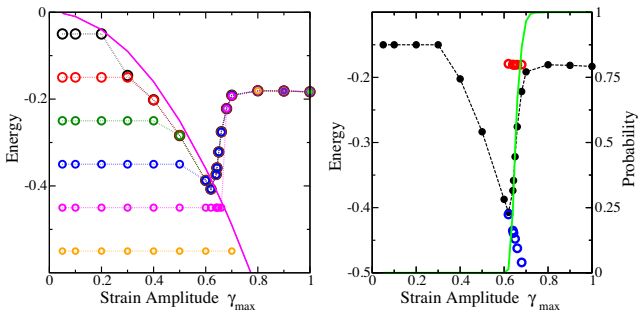

FIG. 2. (Left) The yielding diagram that shows the steady state energies reached after repeated cyclic deformation, as a function of the strain amplitude $\gamma_{\max}$, for a range of initial energies. (Right) Along with average energies over all samples (black), partial average energies are shown, of samples that yield (red) and those that do not (blue), revealing the discontinuous nature of the transition to the yielded state. The yielding probability vs strain is also shown (green).

energy values, energies shift to lower energies, toward a threshold value common to a range of initial energies, before a discontinuous transition occurs, after which the energies follow a common branch regardless of initial energy values. For initial energies lower than the threshold, there is no change vs $\gamma_{\max}$ till a yield value is reached, at which a discontinuous jump in energy is seen. Naturally, the discontinuity in energy grows with the reduction of the initial energy. From Fig. 2(a), the discontinuous nature of the transition is not fully apparent. To reveal it more clearly, for any choice of $\gamma_{\max}$, the final energies for the cases where a transition occurs (and those for which it does not) are computed, as also the probability of occurrence of the transition vs $\gamma_{\max}$. The typical behavior is illustrated (for $E_0^{\text{init}} = -0.15$) in Fig. 2(b), which shows that (i) the yielding probability rises sharply from 0 to 1 in a very narrow range of $\gamma_{\max}$, and (ii) the energy averaged over cases where a transition does not occur continues to decrease with $\gamma_{\max}$ even beyond the yield strain range, whereas when a transition occurs, a nearly constant final energy is reached. The latter observation, interestingly, echoes simulation results [21] where continued annealing is observed beyond the yield strain amplitude, away from the shear band in which strain gets localized. The results here should be interpreted suitably by noting that the present system represents the behavior of one mesoscale block in a more extended system. From the results here, the post-yield energy does not continue to increase, whereas in simulations, it does. This can similarly be interpreted as a result of a larger fraction of the simulated system undergoing yielding rather than a change in the typical energy within that subvolume. Results in [21] clearly support such an interpretation.

Next, the typical variation of energies vs cycle number, averaged over samples for $\gamma_{\max}$ below the yield value, are shown in Fig. 3 for an initial energy of $E_0^{\text{init}} = -0.15$. The timescales (measured in terms of cycles) to reach the final state increase with $\gamma_{\max}$ consistently with simulation results

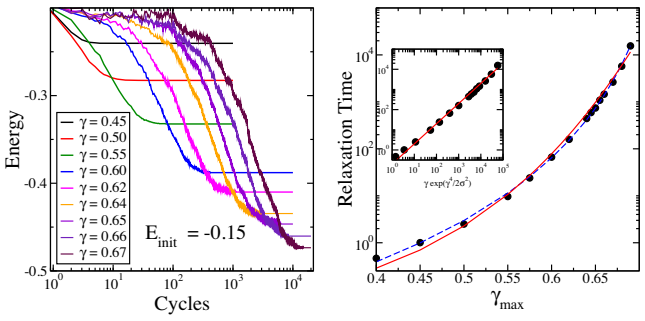

FIG. 3. (Left) Average energies as a function of the number of cycles. (Right) Relaxation time τ to reach the steady state below yielding. The dashed line is a power law fit, and the solid line describes $\tau = A\gamma_{\max}\exp(\gamma_{\max}^4/2\sigma^2)$. The inset shows a log-log plot of τ vs $\gamma_{\max}\exp(\gamma_{\max}^4/2\sigma^2)$.

[11,22], and can be fitted to a power law as shown, but the fit parameters are not meaningful. A way of understanding the increasing timescales is presented below, which leads to the expectation that $\tau \sim \gamma_{\max}\exp(\gamma_{\max}^4/2\sigma^2)$ which provides a very reasonable description. No long relaxation times are observed above the transition, which I interpret to indicating that the long relaxation times observed in simulations arise from parts of the system outside the yielded region rather than the yield region itself, which can be tested in simulations.

Before discussing the results further, I consider variations of the model described above. The first is the regular model discussed above, but with a constraint on the range of energy change when a mesostate transition occurs (with the choice $\delta E = 0.05$, $\sigma = 0.1$, $\mu = 1.1$). The second is the uniform model ($\sigma = 0.1$, $\mu = 1.1$) with γ_0 values uniformly distributed, rather than discretely, for any E_0. I also consider the regular case with $\sigma = 0.15$, $\mu = 1.1$. Finally, with $\mu = 2$, which permits transitions to mesostates of any energy (since the threshold energy for all states is 0), and with the additional condition that the γ_0 value for the new state is the current value of strain, one realizes a specific instance that is the same as the SGR model [26]. The relevant yielding diagrams are reported in Fig. 4. Investigation of these variations reveals that qualitatively, each of them reproduces the behavior discussed above. Equally importantly, these variations do change the threshold energy as well as the energy beyond yielding, which may be relevant in understanding material specific behavior. The constrained case demonstrates that transitions to widely different states is not a necessary feature to produce

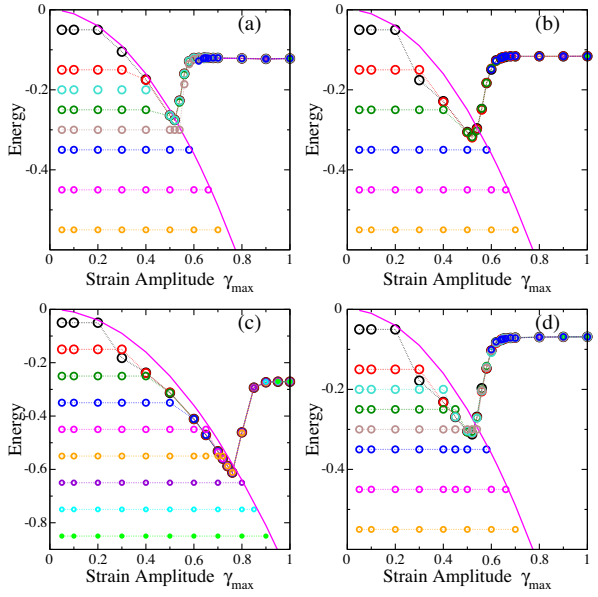

FIG. 4. Yielding diagram for different cases: (a) The *constrained* case with $\delta E = 0.05$, $\sigma = 0.1$, $\mu = 1.1$. (b) The uniform case with $\sigma = 0.1$, $\mu = 1.1$ (c) The regular case with $\sigma = 0.15$, $\mu = 1.1$ (d) The SGR version, with $\sigma = 0.1$, $\mu = 2$.

the observed behavior. The regular case with $\sigma = 0.15$ illustrates that the distribution $P_0(E_0)$ has a strong bearing on the threshold energy. Importantly, it also suggests that models with trivial (e.g., flat) distributions of energies are unlikely to capture the yielding transition under athermal cyclic shear, which should be tested. In the present formulation, limit cycles associated with memory effects [25,34] do not arise. Constructing suitable transition graphs [25,35,36] that can describe such limit cycles needs to be explored.

The most intriguing result here and in earlier simulations is the presence of a threshold energy, which is not an obvious part of the model description. In contrast, the mean energy beyond yielding has a simple explanation, as the energy above which the mean energy to which a mesostate transitions is lower, whereas below, it is higher. To investigate the meaning of the threshold energy, I consider the distribution of final energies that would be reached at the end of a *single* cycle of strain for a given strain amplitude $\gamma_{\max}$, as a function of the initial energy, for the uniform case with $\mu = 1.1$, with initial $\gamma_0 = 0$. Such two dimensional distributions $P(E_0, E_1)$ are shown for a series of $\gamma_{\max}$ values in Fig. 5. For any $\gamma_{\max}$, there is trivially a range of initial energies for which no transition takes place given by $E_0 < -\gamma_{\max}^2$ since the stability range $\gamma_\pm = \gamma_0 \pm \sqrt{-E_0}$. But for higher energies, the transition probabilities are seen to be roughly independent of the initial energy (though this feature is not common to all the cases studied, behavior in other cases is qualitatively the same). It can be seen that the probability to transition to an energy below the threshold for the given strain ($= -\gamma_{\max}^2$, indicated by horizontal red lines) decreases dramatically with an increase in $\gamma_{\max}$, and, between $\gamma_{\max} = 0.5$ and 0.7, it drops strongly (the strain at which the yielding probability is 1/2 in this case is ≈0.563). Thus, the probability to transition to the yielded state becomes overwhelming, although it is never equal to 1. Correspondingly, the probability to transition to the yielded state upon several repeated cycles becomes a sharper function, but moves to higher strain values.

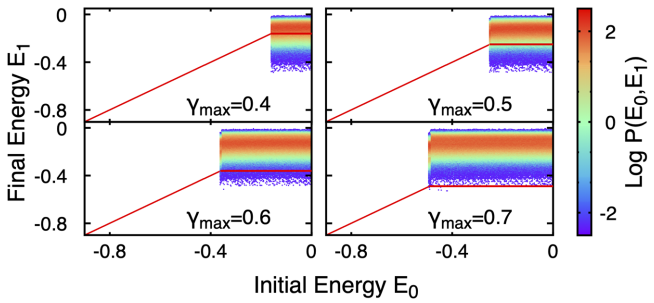

FIG. 5. The histogram of energies reached after one cycle (y axis) vs the initial energy (x axis) for a range of strain amplitudes $\gamma_{\max}$ indicated in the panels, for the uniform case with $\mu = 1.1$. The yield $\gamma_{\max}$ in this case is ≈0.563.

Keeping in mind the case when $\mu = 2$ wherein an unstable mesostate can make a transition to any other mesostate without restriction, a simple, if approximate estimate of the transition probability to yielding can be made as follows. Since the stability range for a state of energy $-E_0$ is $2\sqrt{-E_0}$, over a cycle of strain (or any unit of strain), the transition rate out of that state is inversely proportional to $\sqrt{-E_0}$, and the probability to transition to a new state of energy E' is $P_0(E')$. If one assumes that as a result of these transitions, a stationary distribution of reached within a single cycle, the stationary distribution is given by $P_{\rm st}(E_0) \propto \sqrt{-E_0}P(E_0)$. This is inaccurate for low energies, and also does not incorporate the fact that once an energy below $-\gamma_{\max}^2$ is reached, no further transitions occur. Nevertheless, it is a good approximate description of the distribution of energies reached after one cycle. One can evaluate the probability, after one cycle, of getting trapped in a minimum that is stable at $\gamma_{\max}$, $p_{\rm trap}(\gamma_{\max}) \approx \int_{-\infty}^{-\gamma_{\max}^2} P_{\rm st}(E_0)dE_0 = \Gamma(\frac{3}{4}, \gamma_{\max}^4/2\sigma^2)/\Gamma(\frac{3}{4}) \sim \exp(-\gamma_{\max}^4/2\sigma^2)/\gamma_{\max}$. The relaxation time should go inversely as $p_{\rm trap}$, $\tau \sim \gamma_{\max}\exp(\gamma_{\max}^4/2\sigma^2)$, which was seen to be good description of the simulated results [Fig. 3(b)]. Writing the probability after $N_{\rm cyc}$ cycles to yield as $p_{\rm trans} = (1 - p_{\rm trap})^{N_{\rm cyc}} \sim \exp(-p_{\rm trap}N_{\rm cyc})$ we see that the $p_{\rm trans}$ will be an increasingly sharp function of $\gamma_{\max}$ and the yield strain amplitude, $\gamma_{\max}^Y \sim [\log(N_{\rm cyc})]^{1/4}$, depends very weakly on $N_{\rm cyc}$. Whether interactions between mesoscale regions in a macroscopic sample could lead to a sharp transition needs to be investigated. In [13], it was observed that the threshold energy closely corresponds to the energy at which the average index of saddle points goes to zero, marking a change in the character of the energy landscape. The implications of such a qualitative change, and how it may be incorporated in the present description, merits further investigation.

In summary, the yielding behavior under athermal cyclic deformation has been investigated for a family of models envisaged to represent a mesoscopic system, which remarkably captures several key observations for model glasses that have been investigated through computer simulations using athermal quasistatic cyclic shear (see also [37,38]). The mechanism for the transition is a competition of the stability against cyclic shear of low energy mesostates, and the *entropic* drive associated with the large number of higher energy minima present, reminiscent of arguments presented in [7,9]. The transition is always discontinuous, as also noted for uniform shear in a recent theoretical analysis [16]. These suggest that such a description, embedded in an elastoplastic scheme is suitable for further investigation as an approach to modeling the larger length scale behavior of sheared amorphous solids, such as the emergence of permanent or multiple shear bands [39]. As the approach is based on a local energy landscape description, it has advantages in capturing thermal behavior as well

as athermal behavior. It also suggests detailed investigation of the energetic aspects of local plastic events in simulations [40] in order to understand better how a diversity of amorphous solids may be satisfactorily modeled.

I thank Vishwas Vasisht, Muhittin Mungan, Peter Sollich, Pallabi Das, Monoj Adhikari, Yagyik Goswami, Himangsu Bhaumik, and Surajit Sengupta for comments and help with manuscript preparation, and support through the J. C. Bose Fellowship, SERB, DST, India Grant No. JBR/2020/000015.

*sastry@jncasr.ac.in

[1] D. Bonn, M. M. Denn, L. Berthier, T. Divoux, and S. Manneville, Rev. Mod. Phys. **89**, 035005 (2017).
[2] A. Nicolas, E. E. Ferrero, K. Martens, and J.-L. Barrat, Rev. Mod. Phys. **90**, 045006 (2018).
[3] M. L. Falk and J. S. Langer, Annu. Rev. Condens. Matter Phys. **2**, 353 (2011).
[4] R. Dasgupta, H. G. E. Hentschel, and I. Procaccia, Phys. Rev. Lett. **109**, 255502 (2012).
[5] J. Lin and M. Wyart, Phys. Rev. X **6**, 011005 (2016).
[6] I. Regev, J. Weber, C. Reichhardt, K. A. Dahmen, and T. Lookman, Nat. Commun. **6**, 8805 (2015).
[7] P. K. Jaiswal, I. Procaccia, C. Rainone, and M. Singh, Phys. Rev. Lett. **116**, 085501 (2016).
[8] Y. Jin, P. Urbani, F. Zamponi, and H. Yoshino, Sci. Adv. **4**, eaat6387 (2018).
[9] G. Parisi, I. Procaccia, C. Rainone, and M. Singh, Proc. Natl. Acad. Sci. U.S.A. **114**, 5577 (2017).
[10] P. Urbani and F. Zamponi, Phys. Rev. Lett. **118**, 038001 (2017).
[11] P. Leishangthem, A. D. S. Parmar, and S. Sastry, Nat. Commun. **8**, 14653 (2017).
[12] M. Ozawa, L. Berthier, G. Biroli, A. Rosso, and G. Tarjus, Proc. Natl. Acad. Sci. U.S.A. **115**, 6656 (2018).
[13] H. Bhaumik, G. Foffi, and S. Sastry, Proc. Natl. Acad. Sci. U.S.A. **118**, e2100227118 (2021).
[14] R. Radhakrishnan and S. M. Fielding, Phys. Rev. Lett. **117**, 188001 (2016).
[15] M. Popović, T. W. J. de Geus, and M. Wyart, Phys. Rev. E **98**, 040901(R) (2018).
[16] H. J. Barlow, J. O. Cochran, and S. M. Fielding, Phys. Rev. Lett. **125**, 168003 (2020).
[17] Y. Shi, M. B. Katz, H. Li, and M. L. Falk, Phys. Rev. Lett. **98**, 185505 (2007).
[18] W.-T. Yeh, M. Ozawa, K. Miyazaki, and L. Berthier, Phys. Rev. Lett. **124**, 225502 (2020).
[19] V. V. Vasisht, G. Roberts, and E. Del Gado, Phys. Rev. E **102**, 010604(R) (2020).
[20] N. V. Priezjev, Comput. Mater. Sci. **150**, 162 (2018).
[21] A. D. S. Parmar, S. Kumar, and S. Sastry, Phys. Rev. X **9**, 021018 (2019).
[22] D. Fiocco, G. Foffi, and S. Sastry, Phys. Rev. E **88**, 020301 (R) (2013).
[23] M. Talamali, V. Petäjä, D. Vandembroucq, and S. Roux, C. R. Mec. **340**, 275 (2012).
[24] N. C. Keim, J. D. Paulsen, Z. Zeravcic, S. Sastry, and S. R. Nagel, Rev. Mod. Phys. **91**, 035002 (2019).
[25] M. Mungan, S. Sastry, K. Dahmen, and I. Regev, Phys. Rev. Lett. **123**, 178002 (2019).
[26] P. Sollich, F. Lequeux, P. Hébraud, and M. E. Cates, Phys. Rev. Lett. **78**, 2020 (1997).
[27] E. Jagla, Phys. Rev. E **76**, 046119 (2007).
[28] S. Merabia and F. Detcheverry, Europhys. Lett. **116**, 46003 (2016).
[29] E. Jagla, Phys. Rev. E **96**, 023006 (2017).
[30] This choice, for concreteness, corresponds to the total number of states $\Omega \sim \exp(\alpha N)$, $\alpha \sim 1$ [31] of a subvolume of 50 particles.
[31] S. Sastry, Nature (London) **409**, 164 (2001).
[32] Energies E_0 as well as μ, δE, σ are expressed as dimensionless numbers, scaled to the magnitude of the lowest energy value E_K.
[33] This in principle introduces an additional E_0 dependent in the density of states, but we consider an implementation where the total weight of all relevant mesostates of a given energy is given by $P_0(E_0)$.
[34] M. Adhikari and S. Sastry, Euro. Phys. J. E **41**, 105 (2018).
[35] M. Mungan and T. A. Witten, Phys. Rev. E **99**, 052132 (2019).
[36] D. Fiocco, G. Foffi, and S. Sastry, J. Phys. Condens. Matter **27**, 194130 (2015).
[37] C. Liu, E. E. Ferrero, E. A. Jagla, K. Martens, A. Rosso, and L. Talon, arXiv:2012.15310.
[38] K. Khirallah, B. Tyukodi, D. Vandembroucq, and C. E. Maloney, Phys. Rev. Lett. **126**, 218005 (2021).
[39] V. V. Vasisht, M. L. Goff, K. Martens, and J.-L. Barrat, arXiv:1812.03948.
[40] C. Liu, S. Dutta, P. Chaudhuri, and K. Martens, Phys. Rev. Lett. **126**, 138005 (2021).